Sustained visual priming effects can emerge from attentional oscillation and temporal expectation

Muzhi Wang[1], Yan Huang[2], Huan Luo[1,3], Hang Zhang[1,3,4*]

1. School of Psychological and Cognitive Sciences and Beijing Key Laboratory of Behavior and Mental Health, Peking University, Beijing, China

2. Brain Cognition and Brain Disease Institute for Collaboration Research of SIAT at CAS and the McGovern Institute at MIT, Shenzhen Institutes of Advanced Technology, Chinese Academy of Sciences, Shenzhen, China

3. PKU-IDG/McGovern Institute for Brain Research, Peking University, Beijing, China

4. Peking-Tsinghua Center for Life Sciences, Beijing, China

*Corresponding author:

Hang Zhang, email: hang.zhang@pku.edu.cn

Short title: Oscillated temporal expectation model

Abstract

Priming refers to the influence that a previously encountered object exerts on future responses to similar objects. For many years, visual priming has been known as a facilitation and sometimes an inhibition effect that lasts for an extended period of time. It contrasts with the recent finding of an oscillated priming effect where facilitation and inhibition alternate over time periodically. Here we developed a computational model of visual priming that combines rhythmic sampling of the environment (attentional oscillation) with active preparation for future events (temporal expectation). Counterintuitively, it shows both the sustained and oscillated priming effects can emerge from an interaction between attentional oscillation and temporal expectation. The interaction also leads to novel predictions such as the change of visual priming effects with temporal expectation. Reanalysis of two published datasets and the results of one new experiment of visual priming tasks provide support for the model's relevance to human behavior.

Keywords: visual attention, visual priming, response time, behavioral oscillation, temporal expectation, temporal uncertainty

Introduction

Prior encounter with an object may speed up one's response to a similar object, a pervasive phenomenon in human cognition known as priming (Schacter and Buckner, 1998; Tulving and Schacter, 1990). The visual priming task has proved to be a powerful behavioral paradigm in probing the temporal dynamics of human attention (Eimer and Schlaghecken, 2003). In its simplest version (Fig. 1A), participants judge the pointing direction of a target arrow preceded by a congruent or incongruent prime. The priming effects—response time (RT) for incongruent trials minus RT for congruent trials—may vary with the prime-to-target delay ("SOA"). Classic findings include sustained positive priming in unmasked priming tasks (Neumann and Klotz, 1994) and transient positive priming followed by sustained negative priming in masked priming tasks (Eimer, 1999; Eimer and Schlaghecken, 1998).

Recently, a theta-band (3–5 Hz) RT oscillation has been separated from these classic priming effects by spectral methods (Huang et al., 2015): RT fluctuates up and down as a function of SOA in cycles of approximately 300 msec, with the peaks of congruent trials accompanied by the valleys of incongruent trials and vice versa (Fig. 1DH). The finding of oscillated priming was a surprise but not entirely unexpected. On one hand, there are clues of oscillated priming in the literature—priming effects may first go up, then down, and up again when SOA goes from 0 to 300 msec (Lingnau and Vorberg, 2005). On the other hand, theta-band behavioral oscillations are widely observed in human perception (Benedetto and Morrone, 2017; Landau et al., 2015; Tomassini et al., 2015; Wutz et al., 2016; see VanRullen, 2016 for a review), which may reflect a rhythmic perceptual sampling of the environment.

We performed additional analysis to confirm that the oscillated priming found in Huang et al. (2015) is not an artifact (Supplemental Fig. S8). Moreover, similar

oscillatory effects in RT (Song et al., 2014) as well as in accuracy (Chen et al., 2017) have been recently reported in spatial cueing tasks, in addition to the classic sustained facilitation or inhibition effects at the cued location (Klein, 2000; Posner and Cohen, 1984).

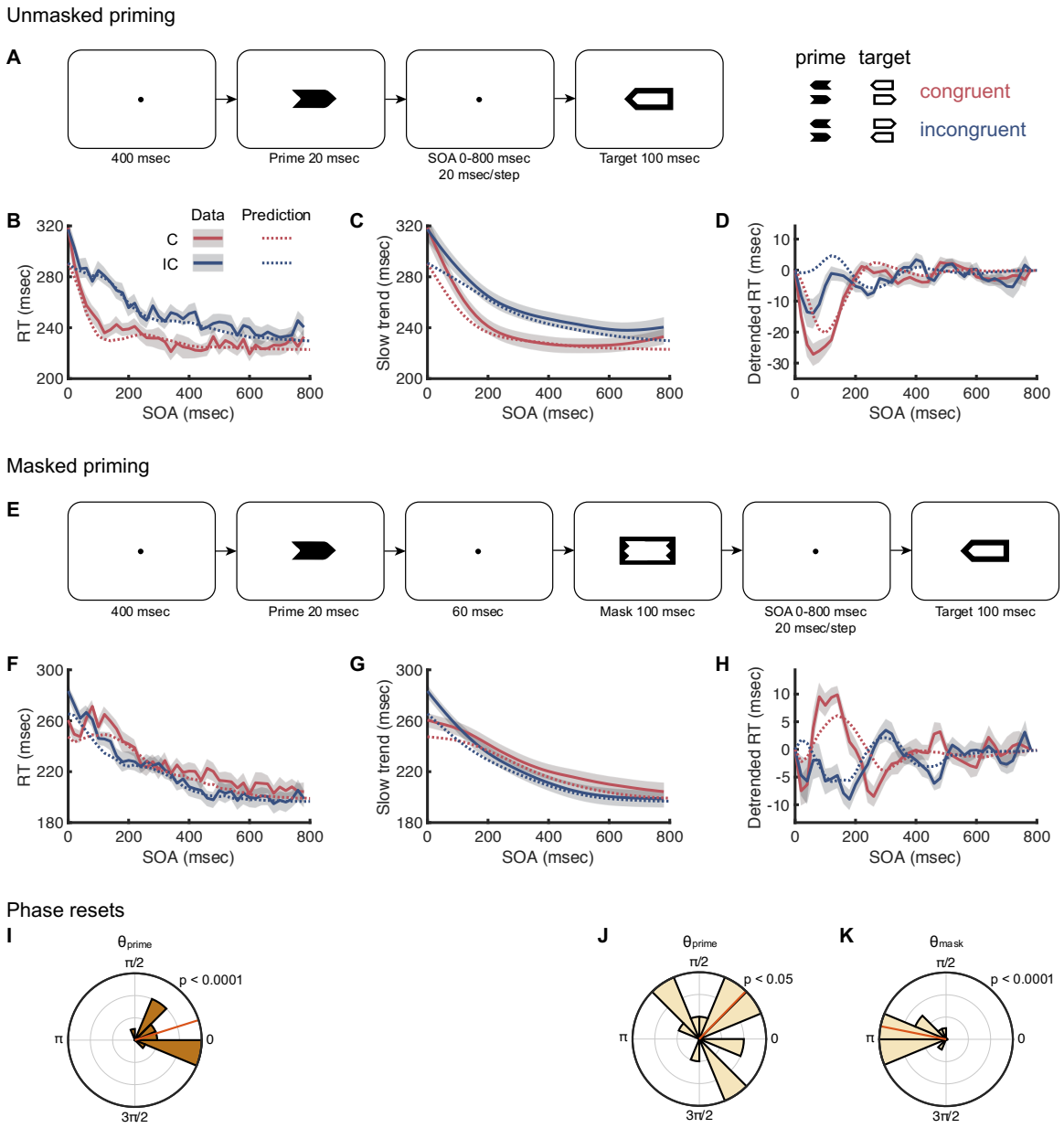

Figure 1. Oscillated Temporal Expectation Model (OTEM) reproduces the three priming effects in Huang et al. (2015). A, unmasked priming task. Participants reported the pointing

direction of the target arrow by key press. When the prime and the target pointed to the same direction, they were congruent (*C*), otherwise incongruent (*IC*). The interval between the prime and the target was referred as SOA. **B,** mean RT as a function of SOA in the unmasked priming task, separately for the congruent (red) and incongruent (blue). Solid lines denote data. Dotted lines denote OTEM predictions. Shadings denote SEM. Following Huang et al. (2015), raw RTs of the unmasked priming task (**B**) were decomposed into slow trends (**C**) and detrended RTs (**D**), where positive priming (**C**) and oscillated priming (**D**) were observed. **E**, masked priming task. The same as unmasked priming task except that a mask followed the prime and the interval between the mask and the target was referred as SOA. **F**, mean RT as a function of SOA in the masked priming task, where positive priming followed by negative priming (slow trends, **G**) and oscillated priming (detrended RTs, **H**) were observed. **I**, Phase of attentional oscillation reset by the prime in the unmasked priming task. **J**, **K**, phases of attentional oscillation reset by the prime and the mask in the masked priming task. θ_{prime} and θ_{mask} were parameters of OTEM estimated from data. Rose plot shows the distribution of θ_{prime} or θ_{mask} across participants, which had significantly coherent values (Rayleigh tests, with *p* values marked on panels). The mean phase (red line) was close to 0 for θ_{prime} and to π for θ_{mask}. That is, attention is biased towards the congruent in the next half cycle following the prime and towards the incongruent in the next half cycle following the mask.

What may explain the coexistence of the classic and oscillated cueing/priming effects, which seem to suggest two conflicting time schedules for attention orienting? Previous theories on spatial cueing (Klein, 2000; Nobre and Rohenkohl, 2014) or visual priming (Bowman et al., 2006; Eimer and Schlaghecken, 2003; Huber, 2014; Lleras and Enns, 2004; Sumner, 2007) have been devoted to the classic effects, which apparently cannot predict any ongoing oscillations. To explain the oscillatory RT effects, an attentional oscillation mechanism seems to be necessary. An additional factor that may have a major impact on RT but is largely neglected by previous cueing/priming theories is temporal expectation. Even though the cue/prime is non-informative about the identity of the target, it signals the countdown to the target arrival. Temporal expectation has thus been assumed in the foreperiod task (Los et al., 2014; Los and Van Den Heuvel,

2001; Luce, 1986; Niemi and Näätänen, 1981; Nobre et al., 2007) to account for the decrease of RT with increasing SOA and is likely to explain a similar RT effect in cueing/priming (e.g. Fig. 1BF).

Here we proposed a computational model that introduces attentional oscillation and temporal expectation into the visual priming task to predict the RT patterns. Its basic idea is close to “active sensing” (Lakatos et al., 2013, 2008) that the perceptual system actively predicts and prepares for potential future events (Nobre and van Ede, 2017; Summerfield and de Lange, 2014). Meanwhile, theta-band attentional oscillations provide fine-grained temporal windows of excitation and inhibition for the accumulation of preparedness (van Vugt et al., 2012). We call the model Oscillated Temporal Expectation Model (OTEM), whose key assumptions are illustrated in Figure 2 and unfolded in the Results. In brief, OTEM predicts not only the oscillated priming effect and the decrease of RT with increasing SOA, but also the classic priming effects. That is, sustained positive and negative priming effects can arise as emergent properties of the model, despite that no sustained excitation or inhibition mechanisms are assumed.

We tested OTEM quantitatively by first fitting it to the behavioral datasets of the unmasked and masked priming experiments in Huang et al. (2015) and found that it well reproduced all the priming effects as well as the overall RT patterns. Next, we performed a new experiment to test the functioning of temporal expectation, a key assumption that distinguishes OTEM from previous accounts of visual priming effects (Bowman et al., 2006; Boy and Sumner, 2010; Vorberg et al., 2003). As predicted, the visual priming effects were influenced not only by SOA but also by temporal expectation. Third, we tested two alternative models and found neither of them could reproduce all the priming effects. Last, we showed that OTEM can be extended to predict error rates and atypical priming effects in the literature.

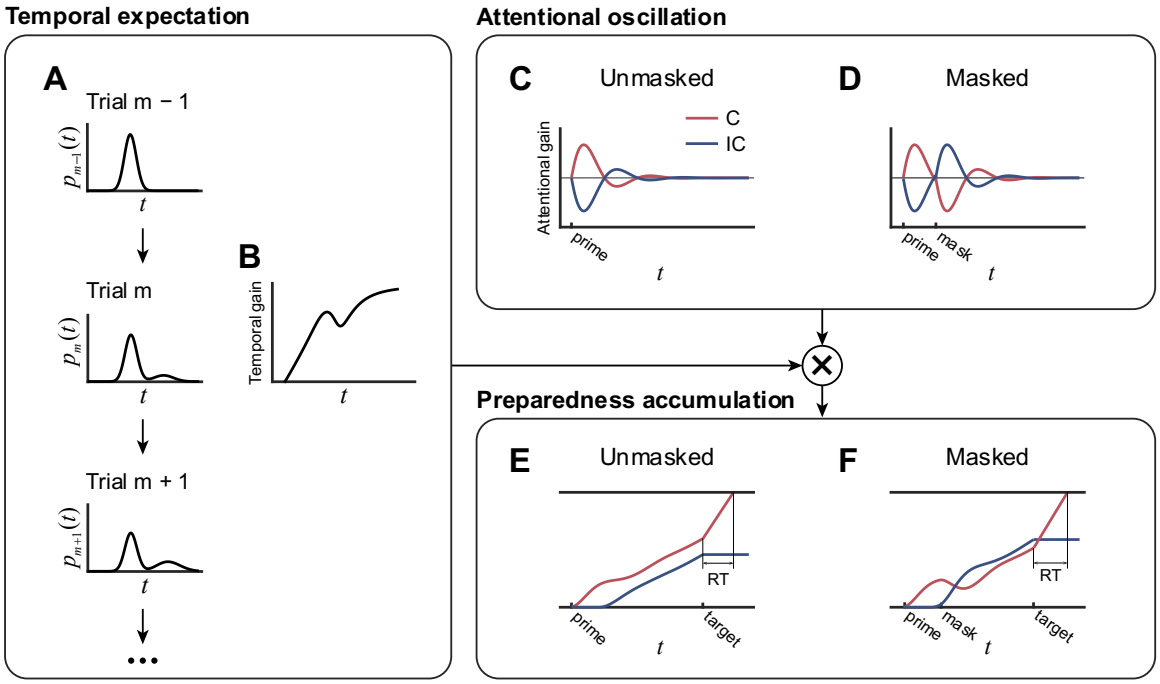

Figure 2. Illustration of the assumptions of OTEM. Temporal expectation: After each trial, the belief of SOA distribution ($p_m(t)$) is updated following the delta rule (**A**). Within a specific trial, the temporal gain (**B**) is computed based on $p_m(t)$ and updated from moment to moment until target onset. **Attentional oscillation**: The attentional gain for the congruent (*C*, in red) and incongruent (*IC*, in blue) oscillates over time, whose amplitude and phase are reset by the prime and the mask (**C**, **D**). **Preparedness accumulation**: Before target onset, two threads of preparedness accumulate over time separately for the congruent and incongruent, with the accumulating speed at each moment determined by the product of the corresponding attentional and temporal gains (**E**, **F**). After target onset, only the thread for the realized target continues to accumulate until it reaches the responding bound. The RT for a specific target is thus determined by the preparedness accumulated for the target up to its onset. Intuitively, the attentional oscillation in the unmasked priming task (**C**) gives the congruent thread a head start in the race (**E**), thus leading to sustained positive priming. In contrast, the mask in the masked priming task resets attentional oscillation (**D**) and reverses the ranking of the congruent and incongruent threads (**F**), thus leading to transient positive priming followed by sustained negative priming.

Results

Oscillated Temporal Expectation Model (OTEM)

The key assumptions of OTEM (Fig. 2) is specified below (see Methods for details). For fluency of presentation, we only briefly describe their motivations here and leave a full treatment of the justification and implications of the assumptions to the Discussion.

Preparedness accumulation. We assume that responses are generated by an accumulation-to-bound process analogous to the racing models of perceptual decision-making (Luce, 1986). After the onset of the prime, two threads of preparation are separately accumulated for the two prospective targets—the congruent and incongruent—until the target arrives (Cisek, 2007; Cisek and Kalaska, 2010), after which only the preparedness for the realized target continues to accumulate. A response occurs when the responding bound is reached. The response time for a specific target is thus determined by the preparedness accumulated for the target up to its onset.

Temporal expectation. We assume that a belief of SOA distribution is learned from past trials following the delta rule (Rescorla and Wagner, 1972). On each trial, the brain uses this distribution as its (probabilistic) temporal expectation for the SOA of the incoming target and, as time elapses, keeps updating the expectation of remaining time until the target appears (de Lange et al., 2013; McGuire and Kable, 2013).

At any specific moment, the temporal expectation—a probability distribution over all future time points—decides how urgent the brain should prepare for prospective targets. To map the influence of the distribution to a single value, we introduce an economic concept: temporal discounting—the longer the expected delay of a reward, the lower the reward is valued in the brain (Frederick et al., 2002; Kable and Glimcher, 2007). In our case, it implies that the expected probability of target onset at a time point in the farther future has a smaller influence on the current preparing rate. Analogous to

170 the application of temporal discounting in the reinforcement learning literature (Sutton
171 and Barto, 1998), we assume that the preparing rate at a specific moment is proportional
172 to the *temporal gain* at the moment, defined as the expected sum of the temporally
173 discounted values of all future probabilities.

174 **Attentional oscillation.** There is increasing evidence that visual attention is a periodic
175 process that sequentially samples different alternatives in the theta frequency range
176 (Fiebelkorn et al., 2013; Kienitz et al., 2018; Landau et al., 2015; Landau and Fries,
177 2012; Song et al., 2014; Tomassini et al., 2015; VanRullen, 2016). Following these
178 empirical findings, we assume that the focus of attention switches gradually between the
179 two prospective targets in theta-band oscillations, leading to anti-phased attentional
180 gains for the congruent and incongruent. The phase of the attentional oscillation is reset
181 by the prime and the mask, while its amplitude decreases exponentially with time, as
182 suggested by stimulus-induced resets of theta-band neuronal oscillations (Buzsáki,
183 2006; Makeig et al., 2002; McCartney et al., 2004; Rizzuto et al., 2003; Tesche and
184 Karhu, 2000) and behavioral oscillations (Fiebelkorn et al., 2013; Landau and Fries,
185 2012; Song et al., 2014). We assume that the preparing rate for the congruent or
186 incongruent target is scaled by its attentional gain as well as by the temporal gain.
187

188 **OTEM reproduces both the classic and oscillated priming effects**

189 The datasets of Huang et al. (2015) include one unmasked and one masked priming
190 experiments (Fig. 1), where RTs for the congruent and incongruent varied as functions
191 of SOA. Fifty different SOAs were sampled for each experiment, in a 20-msec step from
192 0 to 980 msec. Decomposing each raw RT curve into a slow trend and a detrended
193 curve, Huang et al. (2015) identified the classic and oscillated priming effects
194 respectively in the two components.

Given that the oscillated priming effect was the motive of our work, we performed additional analyses on these datasets to confirm that the oscillation was not an artifact from spectral analysis. It was noted that the specific moving-window detrending procedure used by Huang et al. (2015), with its edge artifact, might cause illusory theta-band oscillations in the detrended curve when it was applied to a simulated exponentially-decreasing RT curve without any oscillations. Simulations (Supplemental Fig. S8AB) show that the illusory theta-band oscillations would be eliminated if an exponential curve fitting were used for detrending. In contrast (Supplemental Fig. S8CD), the oscillated priming effect was still present when we applied the same exponential detrending procedure to the datasets of Huang et al. (2015).

We fit OTEM to the RTs of individual trials for correct responses for each participant using maximum likelihood estimates (see Supplemental Fig. S5 for the estimated parameters) and plot the model predictions against data (Fig. 1BF, dotted vs. solid curves). The OTEM predictions captured the following patterns of the observed RT curves. First, the slow trends for both the congruent and incongruent trials decreased monotonically with SOA at a decreasing speed. Second, in the slow trends of the unmasked priming task (Fig. 1C), positive priming (i.e. incongruent RTs above congruent RTs) persisted throughout all SOAs, with the difference between the incongruent and congruent RTs first increasing then decreasing. Third, in the slow trends of the masked priming task (Fig. 1G), positive priming occurred for short SOAs (< 100 msec) and changed into negative priming (i.e. congruent RTs above incongruent RTs) for longer SOAs. Fourth, the detrended RT curves (Fig. 1DH) oscillated at frequencies of 3–5 Hz and were anti-phased for the congruent and incongruent (see the Figs. 2 and 3 of Huang et al. (2015) for the observed frequency spectra and phase differences, and see Supplemental Fig. S1 for OTEM predictions).

In other words, OTEM reproduces both the classic and oscillated priming effects. Given that theta-band attentional oscillations are assumed in OTEM, it is probably not surprising the model can predict the observed oscillated priming. However, the classic positive and negative priming are emergent properties of the model, since no persistent attentional biases towards the congruent or incongruent have been assumed. That is, these classic priming effects arise also from the attentional oscillations. According to the phase parameters estimated from data (Fig. 1IJK), both the prime and the mask induced phase resets that were coherent across participants (Rayleigh test: unmasked prime, r = 0.82, z = 10.87, $p < 0.0001$; masked prime, r = 0.41, z = 2.98, p = 0.049; masked mask, r = 0.89, z = 14.18, $p < 0.0001$). On average, the prime reset the phases of the attentional gains for the congruent and incongruent oppositely to approximately 0 and π (in sine), so that the preparedness of the congruent would accumulate faster than the incongruent in the first half cycle. Conversely, the mask reset the congruent and incongruent phases to approximately π and 0, giving the incongruent an advantage in the subsequent half cycle.

Here is an intuition how the classic priming effects emerge from OTEM (see Fig. 2 for illustrations): After the attentional oscillations are reset by the prime, the specific phase difference allows the attentional gain of the congruent to climb to the peak earlier than that of the incongruent, giving the congruent a lead in preparedness. For unmasked priming tasks, the congruent keeps the lead throughout the race despite that the congruent and incongruent receive alternating advantages in attentional gains, and thus positive priming is observed. For masked priming tasks, a second reset of the attentional oscillations by the mask reverses the lead, resulting in early positive priming and late negative priming.

The emergence of the classic priming effects from OTEM is insensitive to the choice of most parameters in OTEM. Except for the phase reset parameters, changing

246 the parameters of OTEM would only alter the overall RT and the magnitudes of the
247 priming effects but hardly the qualitative finding of the priming effects (Supplemental Fig.
248 S9).

249 **OTEM predicts the effects of temporal expectation**

250 OTEM predicts that the RT of a trial should depend not only on its SOA (i.e. the actual
251 moment of target onset), but also on the temporal expectation that is shaped by past
252 trials. We tested this prediction in a new masked priming experiment, which consisted of
253 four experimental conditions that used the same set of SOAs but differed in local
254 temporal contexts. In the 40-SOA condition, 40 different SOAs (0 to 780 msec in a 20-
255 msec step) were repeated in a random order, as in Huang et al. (2015). In the 20-SOA
256 condition, the same 40 SOAs were divided into two blocks—the first 20 SOAs and last
257 20 SOAs, so that the SOA was expected to be within 0–380 msec for the former and
258 within 400–780 msec for the latter. Similarly, the 10-SOA condition had 4 blocks of 10
259 SOAs and the 4-SOA condition had 10 blocks of 4 SOAs, with the order of the blocks
260 counterbalanced across participants. In the same procedure applied to the datasets of
261 Huang et al. (2015), we fit OTEM to the RTs of individual trials for each participant in
262 each condition (see Supplemental Fig. S5 for the estimated parameters) and plot model
263 predictions against data (Fig. 3A).
264

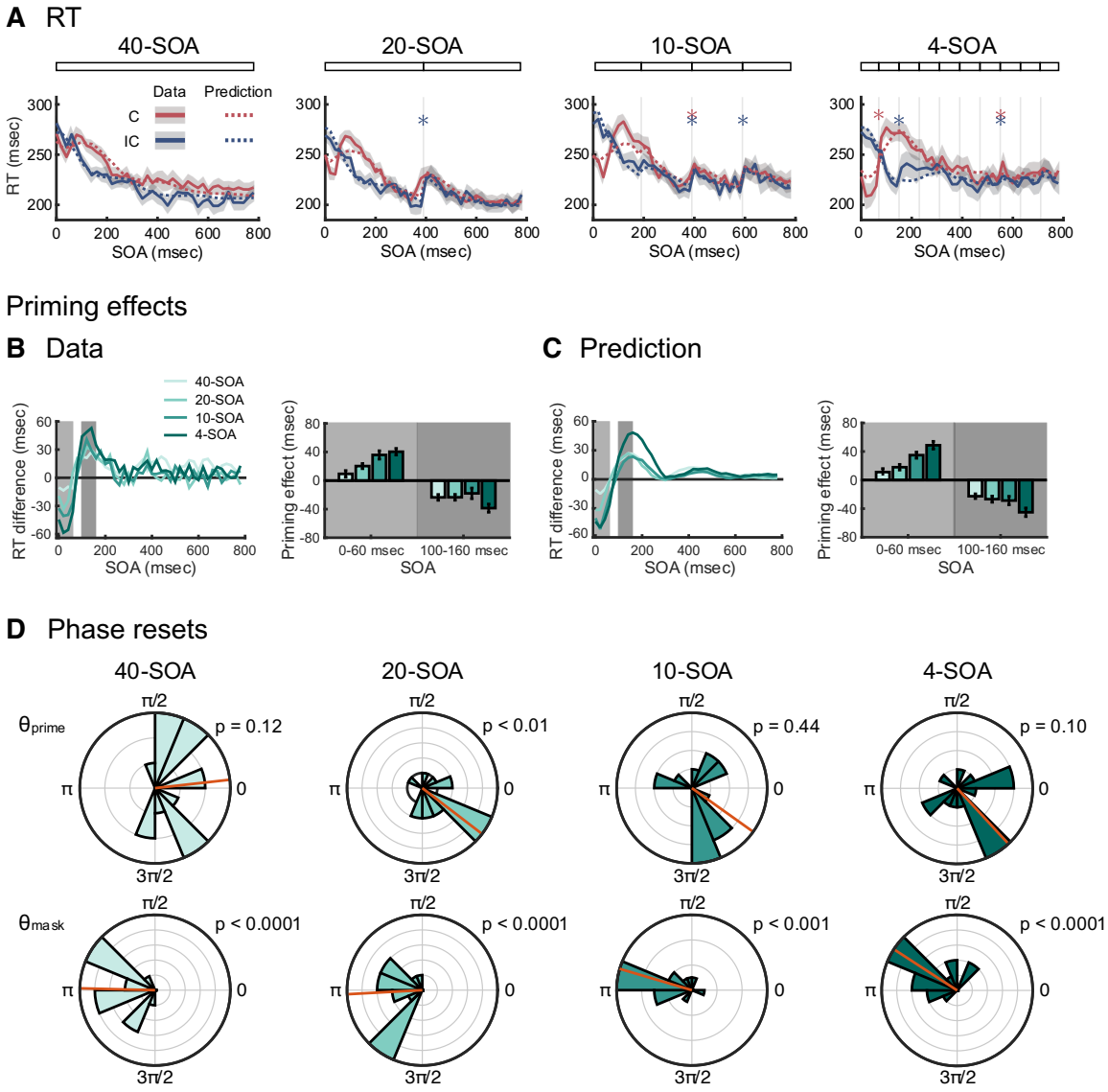

Figure 3. OTEM predicts the effects of temporal expectation in the new experiment. A, mean RT as a function of SOA, separately for the congruent (red) and incongruent (blue). Solid lines denote data. Dotted lines denote OTEM predictions. Shadings denote SEM. Each panel is for one temporal context condition, with the experimental manipulation schematized above the panel (see text). Asterisks indicate statistically significant "jumps" at block borders ($p < 0.05$). **B**, observed priming effects and **C**, OTEM predicted priming effects as functions of SOA. Priming effects were computed as the difference in RT between the congruent and incongruent. Around the peaks of positive priming (light gray shading) and negative priming (dark gray shading), the magnitudes of mean priming effects (bar graphs) increased over the four conditions. **D**, phases of attentional oscillation reset by the prime and the mask. Conventions follow Figure **1I**–**K**. The phases estimated in all four conditions were similar and resembled those of Huang et al. (2015) (see Figure **1I**–**K**).

We found distinctive RT patterns in the four conditions. The 40-SOA condition replicated the results of the masked priming experiment of Huang et al. (2015), including both the classic and oscillated priming effects (Supplemental Figs. S2 & S3), which would serve as a baseline. A hallmark of the other three conditions was a “jump” in RT at the border of two adjacent blocks, for example, the dramatic increase of RT from SOA=380 msec to SOA=400 msec in the 20-SOA condition. Out of the 26 block borders (separately for the congruent and incongruent) of the three conditions, 8 had significant RT increases (one-tailed *t*-tests, *p*s < 0.05). In contrast, there was only one significant RT increase out of the 22 comparisons for the same SOA pairs in the 40-SOA condition (8/26 was significantly higher than 1/22 by Fisher’s exact test, $p = 0.028$).

The OTEM predictions agreed well with the observed RT patterns (Fig. 3A). In particular, OTEM could predict the dramatic increase of RT at the borders of SOA blocks, although it makes no special assumptions about SOA blocks. According to OTEM, the closer the time approaches the last SOA of the block, the sooner the target is expected to arrive, the faster the accumulation of preparedness. Thus, the last SOA of a block could have a faster RT than the first SOA of its next block, despite the general decreasing trend of RT with SOA due to preparedness accumulation.

The magnitudes of priming effects differed across the four conditions (Fig. 3B). Around the peak of positive priming (SOA = 0–60 msec), the mean priming effect (RT difference between the incongruent and congruent) went larger and larger from 40-SOA, 20-SOA, 10-SOA to 4-SOA (one-way ANOVA, $F(3,60) = 13.02$, $p < 0.001$). The mean peaked negative priming effect (SOA = 100–160 msec) exhibited a similar pattern ($F(3,60) = 3.81$, $p = 0.014$). Both patterns were predicted by OTEM (Fig. 3C).

When the raw RT curve was decomposed into a slow trend and a detrended curve as in Huang et al. (2015), the detrended curves of the congruent and incongruent

were close to anti-phased for the 40-SOA condition (though insignificant) but not anti-phased for the 20-SOA, 10-SOA, and 4-SOA conditions. We conjectured that the seemingly absence of anti-phasedness in the latter conditions was due to a failure of the detrending procedure on “jumpy” curves (Supplemental Fig. S2) instead of a real difference in oscillated priming. Consistent with our conjecture, OTEM—where attentional oscillation is assumed to be anti-phased for the congruent and incongruent—well predicted the observed phase differences in the detrended curves for all but the 4-SOA condition (Supplemental Fig. S3).

In addition, the estimated phase parameters in OTEM (Fig. 3D) were indistinguishable across the four conditions (Watson-Williams test, $F(3,60) = 1.11$, $p = 0.35$ for prime phase; $F(3,60) = 2.08$, $p = 0.11$ for mask phase) and resembled those of the masked priming experiment in Huang et al. (2015). That is, the attentional oscillations were not influenced by the temporal context of the experiment.

OTEM predicts that sequential effects would arise from the trial-by-trial updating of temporal expectation. When the preceding trials have longer SOAs, the temporal expectation for the current SOA would be longer, thus the preparing speed would be lower, resulting in a longer RT. We tested this prediction by regressing the current RT over the SOAs of the last three trials, with the RTs of the last three trials and the current SOA serving as nuisance covariates. As predicted, the coefficients for the last and sometimes up to the third last SOA were significantly greater than zero (Fig. 4A), with the patterns of the data closely following those of the model prediction (Fig. 4B).

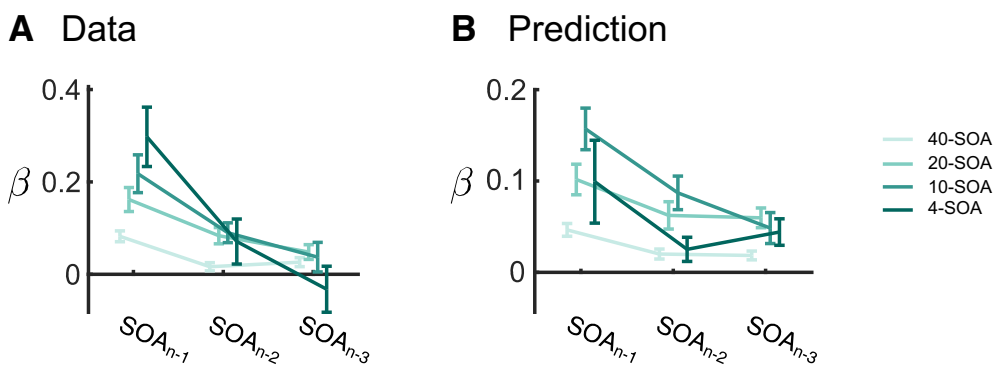

Figure 4. Sequential effects of SOAs. OTEM predicts that when the preceding trials have longer SOAs, the temporal expectation for the current SOA would be longer, thus the preparing speed would be lower, resulting in a longer RT. To quantify this possible sequential effect, we regressed the current RT over the SOAs of the last three trials, with the RTs of the last three trials and the current SOA serving as nuisance covariates. The regression coefficients (β) predicted by OTEM (**B**) closely resembled the patterns of the data (**A**).

OTEM outperforms alternative models

We considered two alternative computational models that can produce visual priming effects. Among them, the "constant accumulation model" was based on the accumulator model of Vorberg et al. (2003). The original model, applying only to unmasked priming tasks to explain positive priming, assumes that the prime triggers a constant-speed accumulation of a decision variable towards the congruent. In the constant accumulation model, we extended the model to masked priming tasks with the additional assumption that the mask would change the direction of the constant accumulation towards the incongruent, so that it can produce negative as well as positive priming effects.

A second alternative model was motivated by a widely-accepted idea in the foreperiod task (Luce, 1986; Niemi and Näätänen, 1981; Nobre et al., 2007) that RT for a delayed target depends on the urgency of response at target onset: The higher the urgency, the shorter the RT. In particular, urgency is defined by hazard rate, that is, the conditional probability the target is expected to occur at the next moment, given that it

348 has not occurred yet. To account for oscillated priming, attentional oscillation is assumed
349 as in OTEM. We call the model “oscillated urgency model”, whose assumptions are
350 otherwise the same as OTEM except for how temporal expectation influences RT: The
351 preparedness for the congruent or incongruent is proportional to the instantaneous
352 hazard rate instead of being accumulated over time (see Methods).

353 We fit the constant accumulation model and oscillated urgency model to the RT
354 data of Huang et al. (2015) and our new experiment using maximum likelihood
355 estimates, in the same procedure as we fit OTEM. The Akaike information criterion
356 corrected for small samples (Akaike, 1974; Hurvich and Tsai, 1989) was used as the
357 metric of goodness-of-fit and the protected exceedance probability (Rigoux et al., 2014;
358 Stephan et al., 2009)—the probability a specific model outperforms all the other
359 models—was calculated as the group-level measure for model comparison. For all the
360 datasets, OTEM outperformed the other two models in AICc and had protected
361 exceedance probabilities approaching 100% (Supplemental Fig. S6A).

362 The deviation of the constant accumulation model from data was obvious
363 (Supplemental Fig. S6B): By definition, it could only predict two opposing RT trends for
364 the congruent and the incongruent—if one decreases with SOA, the other must increase
365 with SOA, a unique finding of Vorberg et al.’s (2003). In the case both the congruent and
366 incongruent RTs decrease with SOA, as in our datasets and most previous visual
367 priming studies (Eimer and Schlaghecken, 2003; Lleras and Enns, 2004; Sumner, 2007),
368 the constant accumulation model would simply fail. The problem with the oscillated
369 urgency model was its inability to produce an enduring positive or negative priming effect
370 (Supplemental Fig. S6C), though its assumptions of attentional oscillation and temporal
371 expectation are similar to those of OTEM. It is because the emergence of positive and
372 negative priming in OTEM relies on the accumulation of preparedness over time as well
373 as on attentional oscillation and temporal expectation. Without the accumulation, the

374 congruent and incongruent RTs would merely follow the fluctuation of attentional
375 oscillations.
376

377 **Extended OTEM explains error rates and atypical priming effects**

378 The OTEM introduced above only applies to correct responses, which make up
379 approximately 95% of the trials of most visual priming experiments including ours
380 (Eimer, 1999; Eimer and Schlaghecken, 1998; Huang et al., 2015; Schlaghecken and
381 Eimer, 2002; Verleger et al., 2004). The error rates, though small, could be patterned
382 (Supplemental Fig. S7A): In the 4-SOA condition, for example, the error rate of the
383 incongruent was higher than that of the congruent around the peak of positive priming
384 (0–60 msec), while it was the reverse around the peak of negative priming (100–160
385 msec). This cannot be explained by speed-accuracy trade-off, since the accuracy for fast
386 responses was even higher than that of slow responses. Such patterns—positive
387 priming is accompanied by a higher error rate for the incongruent and negative priming
388 by a higher error rate for the congruent—were also observed in previous studies using
389 visual priming tasks (Eimer, 1999; Eimer and Schlaghecken, 1998; Vorberg et al., 2003).
390 To model error responses, we extended OTEM to include an additional decision
391 process after target onset, where the congruent and incongruent accumulators race
392 against and inhibit each other (see Methods). Consistent with the observed patterns, the
393 extended OTEM predicts a higher error rate for the incongruent than the congruent at
394 positive priming and the reverse pattern at negative priming (Supplemental Fig. S7B).
395 The RTs and error rates are not cause and effect, but the effects of a common cause:
396 When one accumulator has achieved a higher preparedness than the other at target
397 onset, the subsequent decision process would be biased towards the leading
398 accumulator. In an unmasked priming task, Vorberg et al. (2003) found that the

congruent RT decreased with SOA but the incongruent RT increased with SOA, which deviated from the typical finding that both the congruent and incongruent RTs decrease with SOA (e.g. Fig. 1B). They also found that error rate increased with SOA. We noticed, however, the SOAs they used were unusually short (no longer than 108 msec), so did all the following studies that had found similar RT patterns (Mattler and Palmer, 2012; Sack et al., 2009). Such short SOAs would be within the first half cycle of the attentional oscillation of OTEM (approximately 300 msec per cycle), where the attentional gain for the incongruent is still low. That is, the increase of RT with SOA for the incongruent and the decrease of RT with SOA for the congruent they observed can be part of oscillated priming. Using the same SOAs as in Vorberg et al. (2003), the extended OTEM can reproduce their RT and error rate patterns (Supplemental Fig. S7C).

411 # Discussion

412 We developed OTEM as a computational model that combines attentional oscillation and
413 temporal expectation to explain visual priming effects in RT and tested it in three human
414 behavioral experiments. OTEM accurately reproduces all three kinds of priming effects—
415 positive priming, negative priming, and oscillated priming, while the alternative models
416 fail to do so. It correctly predicts temporal expectation would influence visual priming
417 effects. It explains not only the averaged priming effects, but also trial-by-trial variations
418 in RT. Most surprisingly, OTEM shows that the classic, sustained positive and negative
419 priming effects can be emergent properties of attentional oscillation and temporal
420 expectation, a prediction that qualitatively holds for a wide range of parameter values
421 (Supplemental Fig. S9).

422 ## Relation to previous theories of visual priming effects

423 What causes the visual priming effects? In the past years, theories with incremental
424 assumptions about a perceptual or motor bias have been proposed to explain the
425 increasingly richer phenomena. Among the three priming effects, positive priming was
426 first discovered, at which time the bias was assumed to be triggered by the prime to
427 favor the congruent (Damian, 2001; Eimer, 1999; Eimer and Schlaghecken, 1998;
428 Neumann and Klotz, 1994; Vorberg et al., 2003). When negative priming was later found
429 in masked priming tasks, self-inhibition of the prime (Bowman et al., 2006; Eimer and
430 Schlaghecken, 2002; Schlaghecken et al., 2007; Schlaghecken and Eimer, 2006) or bias
431 reversed by the mask (Lleras and Enns, 2004; Verleger et al., 2004) was introduced to
432 explain the transition from positive to negative priming when SOA increases. Efforts
433 were also made to reproduce positive and negative priming in computational models
434 (Vorberg et al., 2003), neural network models (Bowman et al., 2006; Sohrabi and West,

2009), or computational models with biologically plausible neural implementations (Huber and O'Reilly, 2003).

The model we propose here does not necessarily conflict with previous theories, in the sense that priming effects are triggered by the prime and the mask (see the next section for more discussions on mask) and unfold over time. Meanwhile, OTEM provides a new perspective for visual priming effects, which is able to accommodate the recent empirical finding of oscillated priming as well as the classic effects.

Almost all previous theories considered the visual priming effects as passively determined by the stimuli. Instead, OTEM implements the idea of active sensing (Lakatos et al., 2013, 2009, 2008; Schroeder et al., 2010; Zion Golumbic et al., 2013): the perceptual system rhythmically samples the congruent and incongruent and adaptively prepares for the prospective targets. OTEM reproduces both the classic and oscillated priming effects by attributing the latter to instantaneous attentional fluctuations and the former to accumulated biases driven by attentional oscillation and temporal expectation.

By explaining the classic priming effects as emergent properties of OTEM, we are not at any position doubting the ecological significance of positive or negative priming. Emergent properties of a system can be important by themselves, just like consciousness is believed to be an emergent property of the brain (Minsky, 1986).

With all three priming effects arising from a common process, OTEM naturally predicts that positive and negative priming are closely related. In agreement with this prediction, Boy and Sumner (2010) showed that both positive and negative priming effects are proportional to the strength of stimulus-response associations: When a novel stimulus-response mapping is used, it takes time to build associations, during which positive and negative priming grow with time at the same pace.

460 OTEM also predicts that the classic priming effects may change with temporal
461 expectations. As found in our new experiment, the magnitudes of positive and negative
462 priming effects differed across the four temporal expectation conditions: higher temporal
463 uncertainty led to smaller priming effects (Fig. 3BC). Similarly, Naccache, Blandin, and
464 Dehaene (2002) found that the classic priming effects would vanish when the arrival time
465 of the target was barely predictable.

466 **Neurobiological motivations for OTEM**

467 OTEM is intended to capture the computational heuristics of the neural computations
468 underlying visual priming effects. The neurobiological motivations for some of its key
469 assumptions, such as attentional oscillation (VanRullen, 2016, 2013) and temporal
470 expectation (de Lange et al., 2013; McGuire and Kable, 2013), have been specified in
471 the Introduction. We describe the others below.

472 OTEM assumes a theta-band attentional oscillation whose phase is reset by the
473 prime and the mask. Spontaneous theta-band neuronal oscillations are fairly common in
474 the human brain and are readily reset by task-relevant stimuli (Rizzuto et al., 2003;
475 Tesche and Karhu, 2000; see Buzsaki, 2006 for a review). Further, the oscillatory
476 entrainment of sensory stimuli is anti-phased for the attended and unattended stimuli
477 (Lakatos et al., 2013). Buzsaki (2006) suggested that theta-band neuronal oscillations
478 serve as synchronizers to integrate information over time. Analogously, the attentional
479 oscillation assumed in OTEM may help to integrate temporal expectations over time.

480 There have been elegant models (Huber and O'Reilly, 2003) on how positive
481 priming may spontaneously transition into negative priming with increased exposure to
482 the prime. For the visual (arrow) priming tasks we treated here, however, negative
483 priming can hardly be explained solely as an effect of the prime, because no negative
484 priming effect has ever been observed in unmasked priming tasks (Huang et al., 2015;

Jaśkowski et al., 2008; Klotz and Wolff, 1995; Vorberg et al., 2003). Moreover, it has been found that a mask would not trigger negative priming unless it shares visual features with the prime (Jaśkowski and Przekoracka-Krawczyk, 2005; Verleger et al., 2004 see the arrow-shaped mask in Fig. 1F for an example). In other words, masks are not passive stimuli that simply render the prime invisible but play an active role in the priming effects.

We therefore assume that the mask resets the attentional oscillation to a different phase than the prime does, in order to explain why positive priming is followed by negative priming in masked priming tasks. The phase reset by the mask is left to be a free parameter in OTEM, which turned out to be highly consistent in all our masked priming experiments and was anti-phased to that of the prime (Fig. 1K & Fig. 3D). That is, the mask reverses the attentional oscillation set earlier by the prime. This phase reverse is analogous to perceptual aftereffect (Webster, 2015), with the visual features of the mask that agree with the prime inhibited and those opposite to the prime activated.

Temporal discounting has been found in human perception and action (Shadmehr et al., 2010) as well as in economic decision-making (Frederick et al., 2002; Kable and Glimcher, 2007). In OTEM, we introduced temporal discounting to characterize the tendency to prepare more intensely for a near-future target compared to a far-future target that is equally likely to occur. When the discounting rate is zero, any future event would be treated as urgent as the present event and temporal expectation would thus be meaningless. On the other extreme, when the discounting rate is infinity, only the present matters, which is effectively the assumption adopted by many previous models including but not limited to the hazard rate model of temporal expectation (Los et al., 2014; Los and Van Den Heuvel, 2001; Luce, 1986; Niemi and Näätänen, 1981; Nobre et al., 2007).

Similar to previous studies on temporal expectation (Bueti et al., 2010; Janssen and Shadlen, 2005; Sharma et al., 2014), we also considered the participant's temporal uncertainty and used Weber's law (Allan, 2001; Gibbon, 1977) to model it, with the Weber fraction parameter set to be a constant estimated from previous research (Jazayeri and Shadlen, 2010). In the presence of temporal uncertainty, the probability of a future event can leak into the present such that the participant would appear to prepare for the future even if she only cared about the hazard rate at the current moment. At first sight, temporal uncertainty seems to play a role interchangeable with temporal discounting, which renders the latter redundant. However, a model with the former alone would predict an increase of RT with increasing temporal uncertainty, other things being the same (Tsunoda and Kakei, 2011), which is opposite to our empirical finding that, in the 20-, 10-, or 4-SOA condition, blocks with longer SOAs tend to have shorter RTs (Fig. 3A), though longer SOAs correspond to larger temporal uncertainty. Therefore, for both theoretical and practical reasons, we chose to include both temporal uncertainty and temporal discounting in OTEM.

OTEM assumes that two threads of perceptual or motor preparations develop in parallel before target onset. Simultaneous preparation for multiple potential actions has been reported in neuronal activities (Cisek, 2007, 2005; Cisek and Kalaska, 2010). Such pre-target preparing activities are largely driven by temporal expectation and can bias the subsequent actions (de Lange et al., 2013; Donner et al., 2009). According to OTEM, visual priming effects in RT arise from pre-target preparation instead of post-target decision (but also see the extended OTEM). It echoes the findings that attentional status (Nunez et al., 2017) or temporal expectation (Jepma et al., 2012) mostly influences the non-decision time instead of decision time in RT.

To avoid introducing too many degrees of freedom into OTEM, some of our assumptions were simplifying. For example, we assumed a transition from oscillatory

dynamics to constant preparedness accumulation for the realized target immediately after target onset. To assume a delayed transition would be more realistic, since it takes time to detect the target. Given that the target appears at central vision with high contrast, such a delay tends to be neglectable and whether to include it or not should have little influence on our conclusions.

Limitations and future directions

Visual priming tasks have various forms: The prime and target are often but not confined to arrows (Bar and Biederman, 1998; Boy and Sumner, 2010; Del Cul et al., 2007; Kiefer and Brendel, 2006; Klotz and Wolff, 1995); the response is typically key press (Bar and Biederman, 1998; Dehaene et al., 1998; Eimer and Schlaghecken, 1998; Jaśkowski et al., 2008), but can also be finger pointing (Schmidt, 2002), foot stepping (Eimer et al., 2002), eye movement (Sereno, 1995) or speech (Ansorge et al., 1998). In theory, OTEM can apply to all these tasks.

That being said, we does not intend to explain all important aspects of visual priming effects, such as how the strength of priming effects is influenced by the features of the prime and target, which has received elegant treatment in other models (Huber and O'Reilly, 2003; Kruijne and Meeter, 2017). Neither do we claim that our model provides an implementation-level explanation for visual priming effects. Our work, in Marr's (1982) term, is between the computational and algorithm levels based on neurobiologically motivated assumptions.

What OTEM provides are computational heuristics about how one common process may give rise to priming effects with various temporal dynamics, which allow us to make quantitative, testable behavioral predictions. Given that OTEM explains both the classic and oscillated priming effects based on attentional oscillation, a future test would be to directly manipulate attentional oscillation and see what happens to the priming

effects. OTEM also predicts how a set of latent variables—temporal gain, attentional gain, and preparedness—may change between and within trials. This would facilitate model-based searches to further understand the neural basis of visual priming.

A coexistence of sustained and oscillated effects has also been found in spatial cueing tasks (see Introduction). More generally, OTEM offers a new perspective that may unify the attention-related classic findings with the increasing evidence for attentional oscillations in visual perception. One future question is, may other attention-related classic phenomena be explained in a similar framework?

Methods

Experiments

We had analyzed data from two published experiments of Huang et al. (2015) and one new experiment (see Results). All experiments used the same apparatus and stimuli. The new experiment had been approved by the ethics committee of Institute of Biophysics at Chinese Academy of Sciences. All participants provided informed consent before the experiment and were paid for their time. Sixty-four young adults (29 male, aged 19–27) participated, with 16 participants assigned to each of the four conditions.

Oscillated temporal expectation model (OTEM)

Preparedness accumulation. We assume that two threads of preparedness are accumulated in parallel for the two potential targets after the prime and before target onset, each of which can be formulated as:

$$\frac{de_{\mathrm{alt},m}(t)}{dt} = \varphi_{\mathrm{alt}}(t)\rho_m(t) - \mu \ , \tag{1}$$

where alt denotes whether the potential target is congruent (C) or incongruent (IC) with the prime, $\boldsymbol{m}$ denotes trial number, $\boldsymbol{t}$ denotes the delay since prime, $\boldsymbol{e_{alt,m}(t)}$ denotes accumulated preparedness, $\boldsymbol{\varphi_{alt}(t)}$ denotes attentional gain, $\boldsymbol{\rho_m(t)}$ denotes temporal gain, $\boldsymbol{\mu}$ is a leaky rate parameter.

We assume $e_{\mathrm{alt},m}(0) = 0$. To avoid premature responses before target onset, an upper boundary is imposed on $e_{\mathrm{alt},m}(0) = 0$. After the target arrives, the preparedness for the target continues to accumulate at a constant rate ν while the other thread stops. The expected RT for Trial m is the duration from target onset ($\tau_{\mathrm{target},m}$) to the moment the preparedness hits the response threshold b:

$$x_{\text{expt},m} = \frac{b - e_{\text{alt},m}\left(\tau_{\text{target},m}\right)}{v} \quad . \tag{2}$$

The observed RT $x_{\text{obs},m}$ is modeled by adding a log-normal noise:

$$\log x_{\text{obs},m} = \log x_{\text{expt},m} + N\left(0, \sigma^2_{\text{noise}}\right). \tag{3}$$

<u>Attentional gain</u>. We assume that the attentional gains for the two alternative targets add up to 2 and oscillate anti-phased over time, with the amplitude of oscillation decaying exponentially with time (Fig. 2CD). We define

$$\psi(t) = \begin{cases} \exp\left(-\kappa t\right)\sin\left(2f\pi t + \theta_{\text{prime}}\right), & t < \tau_{\text{mask}}, \\ \exp\left(-\kappa t\right)\sin\left(2f\pi\left(t - \tau_{\text{mask}}\right) + \theta_{\text{mask}}\right), & t \geq \tau_{\text{mask}} \end{cases} \tag{4}$$

where κ is a free parameter for decaying rate, f denotes the frequency of attentional oscillation, θ_{prime} and θ_{mask} are free parameters for phases reset by the prime and mask, τ_{mask} denotes the delay of mask. For the unmasked priming task, $\tau_{\text{mask}} \to \infty$. (In the current implementation of OTEM, we defined $t = 0$ and τ_{mask} as the offset times of the prime and mask.) Following the finding that oscillated priming peaks at 3.3 Hz (Huang et al., 2015), we set $f = 3.3$.

The attentional gains for C and IC can be written as

$$\begin{aligned} \varphi_{\text{C}}(t) &= \quad \psi(t) + 1, \\ \varphi_{\text{IC}}(t) &= \quad -\psi(t) + 1. \end{aligned} \tag{5}$$

<u>Temporal gain: trial-by-trial learning</u>. We assume that the participant's temporal expectation for the target is learned from previous experience trial by trial (Fig. 2A) following the delta-rule learning (Rescorla and Wagner, 1972):

$$p_m = p_{m-1} + \alpha\left(p'_{m-1} - p_{m-1}\right), \tag{6}$$

where p_m and p_{m-1} denote the expected distribution of τ_{target} at the beginning of Trial m and $m - 1$, $0 \leq \alpha \leq 1$ is a free parameter for learning rate. The p'_{m-1} denotes the

perceived distribution of τ_{target} on Trial $m-1$, which is a Gaussian distribution around $\tau_{\text{target},m-1}$:

$$p'_{m-1}(t) = \frac{1}{\sqrt{2\pi}\sigma_{\text{Weber}}} \exp\left(-\frac{\left(t - \tau_{\text{target},m-1}\right)^2}{2\sigma_{\text{Weber}}^2} \right), \tag{7}$$

where σ_{Weber} follows Weber's law, $\sigma_{\text{Weber}} = k\tau_{\text{target},m}$ for unmasked and $\sigma_{\text{Weber}} = k\left(\tau_{\text{target},m} - \tau_{\text{mask}}\right)$ for masked priming tasks, with Weber's fraction $k = 0.13$ (Jazayeri and Shadlen, 2010). We set p_1 to be a uniform distribution between the minimum and maximum τ_{target}.

<u>Temporal gain: real-time updating within trial</u>. We assume that within each trial the brain keeps updating its expectation for the arrival time of the target (Fig. 2B). On Trial m, the expected distribution of τ_{target} at Time t ($t < \tau_{\text{target},m}$) is

$$q_m\left(t' \middle| t\right) = \begin{cases} 0, & t' < t, \\ \dfrac{p_m\left(t'\right)}{\int_t^\infty p_m\left(u\right) du}, & t' \geq t. \end{cases} \tag{8}$$

As a special case, the hazard rate of target onset at Time t is $h\left(t\right) = q_m\left(t' = t \middle| t\right)$.

Considering the target as a future reward, we define the temporal gain at Time t as the expectation of the discounted future reward:

$$\rho_m(t) = \int_t^\infty \gamma^{u-t} q_m(u|t) du, \tag{9}$$

where $0 \leq \gamma \leq 1$ is a free parameter for discounting rate.

In total, OTEM has nine parameters for unmasked priming tasks: learning rate, α; temporal discounting rate, γ; leaky rate, μ; decaying rate of oscillation, κ; phase reset by the prime, θ_{prime}; maximum preparedness before target onset, ζ; accumulating rate after target onset, ν; responding threshold, b; standard deviation of log-normal noise,

σ_{noise}. For masked priming tasks, there is one more parameter: phase reset by the mask, θ_{mask}.

Frequency of attentional oscillation

In the model fitting, we had fixed the frequency of attentional oscillation to 3.3 Hz, the observed frequency of oscillated priming. The RTs predicted by OTEM exhibits the same frequency of oscillated priming as that of the assumed attentional oscillation (Supplemental Figs. S1–S3). That is, a theta-band attentional oscillation is sufficient for producing the theta-band oscillated priming.

We also tested whether the 3.3 Hz attentional oscillation is necessary. To do this, we varied the frequency of attentional oscillation, fit the OTEM model for each frequency, and compared their goodness-of-fit (AICc). For computational difficulties, we only considered a limited set of frequencies spanning 2 to 16 Hz. For all three experiments, the AICc first decreased and later increased with the frequency of attentional oscillated, with the best fit occurred at 3.3 or 4 Hz (Supplemental Fig. S4).

Extension of OTEM with a decision process

To explain the patterned errors in visual priming tasks, we enhanced OTEM with an error-prone decision process. The extended OTEM assumes that after target onset both the congruent and incongruent threads continue to accumulate, inhibiting each other and racing to the responding bound. The racing follows the linear ballistic accumulator model (Brown and Heathcote, 2005):

$$\begin{cases} \dfrac{de_{\text{target},m}}{dt} = v_{\text{target}} - \eta e_{\text{other},m}, \\ \dfrac{de_{\text{other},m}}{dt} = v_{\text{other}} - \eta e_{\text{target},m}. \end{cases} \tag{10}$$

where η is a free parameter, v_{target} and v_{other} are accumulating rates for the target and

the other threads. The values of v_{target} and v_{other} on each trial are randomly sampled from Gaussian distributions $N\left(\bar{v}_{\text{target}}, \sigma^2_{\text{target}}\right)$ and $N\left(\bar{v}_{\text{other}}, \sigma^2_{\text{other}}\right)$, with $\bar{v}_{\text{target}} > \bar{v}_{\text{other}}$.

Due to computational difficulties, we did not fit the extended OTEM and focused on qualitative predictions. To simulate for the results of Vorberg et al. (2003), we used the fitted parameters from the 4-SOA condition and manually set the additional parameters for the decision process.

Oscillated urgency model

The oscillated urgency model is the same as OTEM, except that the preparedness for a potential target is not accumulated over time but determined by hazard rate. That is, Eq. 1 is replaced by

$$e_{\text{alt},m} = \varphi_{\text{alt}}(t) h_m(t), \tag{11}$$

where $\varphi_{\text{alt}}(t)$ denotes attentional gain, $h_m(t)$ denotes hazard rate.

In total, oscillated urgency model has 7 free parameters: learning rate, α; decaying rate of oscillation, κ; phase reset by the prime or mask, θ; maximum preparedness before target onset, ζ; accumulating rate after target onset, v; response threshold, b; standard deviation of log-normal noise, σ_{noise}.

Constant accumulation model

The constant accumulation model is based on the accumulator model of Vorberg et al. (2003). The model assumes two accumulators for the two potential targets, the congruent and incongruent. Response is made when the absolute difference between the two accumulators exceeds the response threshold b. The same log-normal noise applies as in OTEM (Eq. 3).

Each accumulator follows

$$\frac{de_{\mathrm{alt},m}(t)}{dt} = -\mu e_{\mathrm{alt},m}(t) + \lambda_{\mathrm{alt}}(t), \tag{12}$$

where μ is a free parameter for growth-decay rate, $\lambda_{\mathrm{alt}}(t)$ denotes the rate of accumulation triggered by the prime, mask, or target as defined below. Following Vorberg et al. (2003), we assume that the prime and target would trigger positive accumulation rates for accumulators in their directions. To account for the observed effect of the mask (i.e. negative priming in masked priming tasks), we further assume that the mask would trigger a negative accumulation rate for the accumulator in the direction of the prime. That is, when the target is congruent with the prime,

$$\begin{aligned} \lambda_{\mathrm{C}}(t) &= \begin{cases} \lambda_s, & 0 \le t < \tau_{\mathrm{mask}}, \\ -\lambda_s, & \tau_{\mathrm{mask}} \le t < \tau_{\mathrm{target},m}, \\ \lambda_s, & \tau_{\mathrm{target},m} \le t, \end{cases} \\ \lambda_{\mathrm{IC}}(t) &= 0. \end{aligned} \tag{13}$$

When the target is incongruent with the prime,

$$\begin{aligned} \lambda_{\mathrm{C}}(t) &= \begin{cases} \lambda_s, & 0 \le t < \tau_{\mathrm{mask}}, \\ -\lambda_s, & \tau_{\mathrm{mask}} \le t < \tau_{\mathrm{target},m}, \\ 0, & \tau_{\mathrm{target},m} \le t, \end{cases} \\ \lambda_{\mathrm{IC}}(t) &= \begin{cases} 0, & t < \tau_{\mathrm{target},m}, \\ \lambda_s, & \tau_{\mathrm{target},m} \le t. \end{cases} \end{aligned} \tag{14}$$

where λ_s is a free parameter, $t = 0$ corresponds to prime onset and τ_{mask} to mask onset. For the unmasked condition, $\tau_{\mathrm{mask}} = \tau_{\mathrm{target},m}$.

The threshold parameter b is redundant and fixed as 1. In total, the model has 4 free parameters: effect of stimulus, λ_s; growth-decay rate, μ; maximum preparedness before target, ζ; standard deviation of log-normal noise, σ_{noise}.

Model fitting and comparison procedures

All the models were fitted on the individual level using the maximum likelihood estimate. We used the interior-point algorithm of the *fmincon* function in MATLAB (MathWorks) to find the parameters that minimized negative log likelihood. To verify that we had found the global minimum, we repeated the search process with different starting points. We used AICc—the Akaike information criterion with a correction for finite sample size (Akaike, 1974; Hurvich and Tsai, 1989)—for model comparison and calculated the protected exceedance probability of the group-level Bayesian model selection (Rigoux et al., 2014; Stephan et al., 2009) as an omnibus measure across participants.

Acknowledgments

YH was supported by Shenzhen Science and Technology Research Funding Program JCYJ20170818161400180 and Guangdong Provincial Key Laboratory of Brain Connectome and Behavior 2017B030301017. HL was supported by National Natural Science Foundation of China grants 31522027 and 31571115. HZ was supported by National Natural Science Foundation of China grants 31571117 and 31871101, and funding from Peking-Tsinghua Center for Life Sciences. Part of the analysis was performed on the High-Performance Computing Platform of the Center for Life Sciences at Peking University and supported by the High-performance Computing Platform of Peking University. The funders had no role in study design, data collection and analysis, decision to publish, or preparation of the manuscript.

References

Akaike H. 1974. A new look at the statistical model identification. *IEEE transactions on automatic control* **19**:716–723. doi:10.1007/978-1-4612-1694-0_16

Allan LG. 2001. Time Perception Models In: Smelser NJ, Baltes PB, editors. International Encyclopedia of the Social & Behavioral Sciences: Second Edition. Oxford: Elsevier. pp. 15696–15699. doi:https://doi.org/10.1016/B0-08-043076-7/00668-9

Ansorge U, Klotz W, Neumann O. 1998. Manual and verbal responses to completely masked (unreportable) stimuli: Exploring some conditions for the metacontrast dissociation. *Perception* **27**:1177–1189. doi:10.1068/p271177

Bar M, Biederman I. 1998. Subliminal visual priming. *Psychological Science* **9**:464–469. doi:10.1111/1467-9280.00086

Benedetto A, Morrone MC. 2017. Saccadic suppression is embedded within extended oscillatory modulation of sensitivity. *Journal of Neuroscience* **37**:3661–3670. doi:10.1523/JNEUROSCI.2390-16.2016

Bowman H, Schlaghecken F, Eimer M. 2006. A neural network model of inhibitory processes in subliminal priming. *Visual Cognition* **13**:401–480. doi:10.1080/13506280444000823

Boy F, Sumner P. 2010. Tight coupling between positive and reversed priming in the masked prime paradigm. *Journal of Experimental Psychology: Human Perception and Performance* **36**:892–905. doi:10.1037/a0017173

Brown S, Heathcote A. 2005. A Ballistic Model of Choice Response Time. *Psychological Review* **112**:117–128. doi:10.1037/0033-295X.112.1.117

741 Bueti D, Bahrami B, Walsh V, Rees G. 2010. Encoding of Temporal Probabilities in the
742 Human Brain. *The Journal of Neuroscience* **30**:4343–4352.
743 doi:10.1523/JNEUROSCI.2254-09.2010
744 Buzsáki G. 2006. Rhythms of the Brain. New York: Oxford University Press.
745 doi:10.1093/acprof:oso/9780195301069.001.0001
746 Chen A, Wang A, Wang T, Tang X, Zhang M. 2017. Behavioral Oscillations in Visual
747 Attention Modulated by Task Difficulty. *Frontiers in Psychology* **8**:1630.
748 doi:10.3389/fpsyg.2017.01630
749 Cisek P. 2007. Cortical mechanisms of action selection: the affordance competition
750 hypothesis. *Philosophical transactions of the Royal Society of London Series B,*
751 *Biological sciences* **362**:1585–1599. doi:10.1098/rstb.2007.2054
752 Cisek P. 2005. Neural representations of motor plans, desired trajectories, and
753 controlled objects. *Cognitive Processing* **6**:15–24. doi:10.1007/s10339-004-0046-7
754 Cisek P, Kalaska JF. 2010. Neural Mechanisms for Interacting with a World Full of
755 Action Choices. *Annual Review of Neuroscience* **33**:269–298.
756 doi:10.1146/annurev.neuro.051508.135409
757 Damian MF. 2001. Congruity effects evoked by subliminally presented primes:
758 Automaticity rather than semantic processing. *Journal of Experimental Psychology:*
759 *Human Perception and Performance* **27**:154–165. doi:10.1037/0096-1523.27.1.154
760 de Lange FP, Rahnev DA, Donner TH, Lau H. 2013. Prestimulus Oscillatory Activity over
761 Motor Cortex Reflects Perceptual Expectations. *The Journal of Neuroscience*
762 **33**:1400 LP-1410. doi:10.1523/JNEUROSCI.1094-12.2013
763 Dehaene S, Naccache L, Le Clec'H G, Koechlin E, Mueller M, Dehaene-Lambertz G,
764 van de Moortele P-F, Le Bihan D. 1998. Imaging unconscious semantic priming.
765 *Nature* **395**:597–600. doi:10.1038/26967

766 Del Cul A, Baillet S, Dehaene S. 2007. Brain Dynamics Underlying the Nonlinear
767 Threshold for Access to Consciousness. *PLOS Biology* **5**:e260.
768 doi:10.1371/journal.pbio.0050260
769 Donner TH, Siegel M, Fries P, Engel AK. 2009. Buildup of Choice-Predictive Activity in
770 Human Motor Cortex during Perceptual Decision Making. *Current Biology* **19**:1581–
771 1585. doi:https://doi.org/10.1016/j.cub.2009.07.066
772 Eimer M. 1999. Facilitatory and inhibitory effects of masked prime stimuli on motor
773 activation and behavioural performance. *Acta psychologica* **101**:293–313.
774 doi:10.1016/S0001-6918(99)00009-8
775 Eimer M, Schlaghecken F. 2003. Response facilitation and inhibition in subliminal
776 priming. *Biological Pyschology* **64**:7–26. doi:10.1016/S0301-0511(03)00100-5
777 Eimer M, Schlaghecken F. 2002. Links between conscious awareness and response
778 inhibition: evidence from masked priming. *Psychonomic bulletin & review* **9**:514–
779 520. doi:10.3758/BF03196307
780 Eimer M, Schlaghecken F. 1998. Effects of Masked Stimuli on Motor Activation:
781 Behavioral and Electrophysiological Evidence. *Journal of experimental psychology*
782 *Human perception and performance* **24**:1737–1747. doi:10.1037/0096-
783 1523.24.6.1737
784 Eimer M, Schubö A, Schlaghecken F. 2002. Locus of inhibition in the masked priming of
785 response alternatives. *Journal of Motor Behavior* **34**:3–10.
786 doi:10.1080/00222890209601926
787 Fiebelkorn IC, Saalmann YB, Kastner S. 2013. Rhythmic sampling within and between
788 objects despite sustained attention at a cued location. *Current Biology* **23**:2553–
789 2558. doi:10.1016/j.cub.2013.10.063

Frederick S, Loewenstein G, O'Donoghue T. 2002. Time Discounting and Time Preference: A Critical Review. *Journal of Economic Literature* **40**:351–401. doi:10.1257/002205102320161311

Gibbon J. 1977. Scalar expectancy theory and Weber's law in animal timing. *Psychological Review* **84**:279–325. doi:10.1037/0033-295X.84.3.279

Huang Y, Chen L, Luo H. 2015. Behavioral Oscillation in Priming: Competing Perceptual Predictions Conveyed in Alternating Theta-Band Rhythms. *The Journal of Neuroscience* **35**:2830–2837. doi:10.1523/JNEUROSCI.4294-14.2015

Huber DE. 2014. The Rise and Fall of the Recent Past: A Unified Account of Immediate Repetition Paradigms In: Ross B, editor. Psychology of Learning and Motivation. Cambridge: Academic Press. pp. 191–226. doi:10.1016/B978-0-12-800090-8.00005-6

Huber DE, O'Reilly RC. 2003. Persistence and accommodation in short-term priming and other perceptual paradigms: temporal segregation through synaptic depression. *Cognitive Science* **27**:403–430. doi:https://doi.org/10.1016/S0364-0213(03)00012-0

Hurvich CM, Tsai C-L. 1989. Regression and time series model selection in small samples. *Biometrika* **76**:297–307. doi:10.1093/biomet/76.2.297

Janssen P, Shadlen MN. 2005. A representation of the hazard rate of elapsed time in macaque area LIP. *Nature Neuroscience* **8**:234–241. doi:10.1038/nn1386

Jaśkowski P, Białuńska A, Tomanek M, Verleger R. 2008. Mask- and distractor-triggered inhibitory processes in the priming of motor responses: An EEG study. *Psychophysiology* **45**:70–85. doi:10.1111/j.1469-8986.2007.00595.x

Jaśkowski P, Przekoracka-Krawczyk A. 2005. On the role of mask structure in subliminal priming. *Acta Neurobiologiae Experimentalis* **65**:409–417.

Jazayeri M, Shadlen MN. 2010. Temporal context calibrates interval timing. *Nature neuroscience* **13**:1020–1026. doi:10.1038/nn.2590

Jepma M, Wagenmakers E-J, Nieuwenhuis S. 2012. Temporal expectation and information processing: A model-based analysis. *Cognition* **122**:426–441. doi:https://doi.org/10.1016/j.cognition.2011.11.014

Kable JW, Glimcher PW. 2007. The neural correlates of subjective value during intertemporal choice. *Nature Neuroscience* **10**:1625–1633. doi:10.1038/nn2007

Kiefer M, Brendel D. 2006. Attentional modulation of unconscious “automatic” processes: Evidence from event-related potentials in a masked priming paradigm. *Journal of Cognitive Neuroscience* **18**:184–198. doi:10.1162/jocn.2006.18.2.184

Kienitz R, Schmiedt JT, Shapcott KA, Kouroupaki K, Saunders RC, Schmid MC. 2018. Theta Rhythmic Neuronal Activity and Reaction Times Arising from Cortical Receptive Field Interactions during Distributed Attention. *Current Biology* **28**:2377–2387. doi:10.1016/j.cub.2018.05.086

Klein RM. 2000. Inhibition of return. *Trends in Cognitive Sciences* **4**:138–147. doi:10.1016/S1364-6613(00)01452-2

Klotz W, Wolff P. 1995. The effect of a masked stimulus on the response to the masking stimulus. *Psychological Research* **58**:92–101. doi:10.1007/BF00571098

Kruijne W, Meeter M. 2017. You prime what you code: The fAIM model of priming of pop-out. *PLoS ONE*. doi:10.1371/journal.pone.0187556

Lakatos P, Karmos G, Mehta AD, Ulbert I, Schroeder CE. 2008. Entrainment of Neuronal Oscillations as a Mechanism of Attentional Selection. *Science* **320**:110–113. doi:10.1126/science.1154735

Lakatos P, Musacchia G, O’Connel MN, Falchier AY, Javitt DC, Schroeder CE. 2013. The Spectrotemporal Filter Mechanism of Auditory Selective Attention. *Neuron* **77**:750–761. doi:10.1016/j.neuron.2012.11.034

841 Lakatos P, O'Connell MN, Barczak A, Mills A, Javitt DC, Schroeder CE. 2009. The
842 Leading Sense: Supramodal Control of Neurophysiological Context by Attention.
843 *Neuron* **64**:419–430. doi:10.1016/j.neuron.2009.10.014
844 Landau AN, Fries P. 2012. Attention samples stimuli rhythmically. *Current Biology*
845 **22**:1000–1004. doi:10.1016/j.cub.2012.03.054
846 Landau AN, Schreyer HM, Van Pelt S, Fries P. 2015. Distributed attention is
847 implemented through theta-rhythmic gamma modulation Published in edited form
848 in: Current Biology. *Current Biology* **25**:2332–2337. doi:10.1016/j.cub.2015.07.048
849 Lingnau A, Vorberg D. 2005. The time course of response inhibition in masked priming.
850 *Perception and Psychophysics* **67**:545–557. doi:10.3758/BF03193330
851 Lleras A, Enns JT. 2004. Negative Compatibility or Object Updating? A Cautionary Tale
852 of Mask-Dependent Priming. *Journal of Experimental Psychology: General*
853 **133**:475–493. doi:10.1037/0096-3445.133.4.475
854 Los SA, Kruijne W, Meeter M. 2014. Outlines of a multiple trace theory of temporal
855 preparation. *Frontiers in Psychology* **5**:1058. doi:10.3389/fpsyg.2014.01058
856 Los SA, Van Den Heuvel CE. 2001. Intentional and unintentional contributions to
857 nonspecific preparation during reaction time foreperiods. *Journal of Experimental*
858 *Psychology: Human Perception and Performance* **27**:370–386. doi:10.1037/0096-
859 1523.27.2.370
860 Luce RD. 1986. Response times: Their role in inferring elementary mental organization.
861 New York, NY: Oxford University Press.
862 Makeig S, Westerfield M, Jung T-P, Enghoff S, Townsend J, Courchesne E, Sejnowski
863 TJ. 2002. Dynamic Brain Sources of Visual Evoked Responses. *Science* **295**:690–
864 694. doi:10.1126/science.1066168
865 Marr D. 1982. Vision: A computational investigation into the human representation and
866 processing of visual information. Cambridge, MA: MIT Press.

867 Mattler U, Palmer S. 2012. Time course of free-choice priming effects explained by a
868 simple accumulator model. *Cognition* **123**:347–360.
869 doi:10.1016/j.cognition.2012.03.002
870 McCartney H, Johnson AD, Weil ZM, Givens B. 2004. Theta reset produces optimal
871 conditions for long-term potentiation. *Hippocampus* **14**:684–687.
872 doi:10.1002/hipo.20019
873 McGuire JT, Kable JW. 2013. Rational temporal predictions can underlie apparent
874 failures to delay gratification. *Psychological Review* **120**:395–410.
875 doi:10.1037/a0031910
876 Minsky M. 1986. The Society of Mind. New York, NY: Simon & Schuster, Inc.
877 Naccache L, Blandin E, Dehaene S. 2002. Unconscious Masked Priming Depends on
878 Temporal Attention. *Psychological Science* **13**:416–424. doi:10.1111/1467-
879 9280.00474
880 Neumann O, Klotz W. 1994. Motor responses to nonreportable, masked stimuli: Where
881 is the limit of direct parameter specification? In: Umiltà C, Moscovitch M, editors.
882 Attention and Performance XV, Attention and Performance Series. Cambridge, MA:
883 MIT Press. pp. 123–150.
884 Niemi P, Näätänen R. 1981. Foreperiod and simple reaction time. *Psychological Bulletin*
885 **89**:133–162. doi:10.1037/0033-2909.89.1.133
886 Nobre A, Correa A, Coull J. 2007. The hazards of time. *Current Opinion in Neurobiology*
887 **17**:465–470. doi:10.1016/j.conb.2007.07.006
888 Nobre AC, Rohenkohl G. 2014. Time for the fourth dimension in attention In: Nobre AC,
889 Kastner S, editors. The Oxford Handbook of Attention. Oxford, UK: Oxford
890 University Press. pp. 676–721. doi:10.1093/oxfordhb/9780199675111.013.036
891 Nobre AC, van Ede F. 2017. Anticipated moments: temporal structure in attention.
892 *Nature Reviews Neuroscience* **19**:34–48. doi:10.1038/nrn.2017.141

Nunez MD, Vandekerckhove J, Srinivasan R. 2017. How attention influences perceptual decision making: Single-trial EEG correlates of drift-diffusion model parameters. *Journal of Mathematical Psychology* **76**:117–130. doi:10.1016/j.jmp.2016.03.003

Posner MI, Cohen Y. 1984. Components of Visual Orienting In: Bouma H, Bouwhuis DG, editors. Attention and Performance X. Hillsdale, NJ: Lawrence Erlbaum Associates. pp. 531–556.

Rescorla RA, Wagner AR. 1972. A theory of Pavlovian conditioning: Variations in the effectiveness of reinforcement and nonreinforcement In: Black AH, Prokasy WF, editors. Classical Conditioning II: Current Research and Theory. East Norwalk, CT: Appleton-Century-Crofts. pp. 64–99.

Rigoux L, Stephan KE, Friston KJ, Daunizeau J. 2014. Bayesian model selection for group studies — Revisited. *Neuroimage* **84**:971–985. doi:10.1016/j.neuroimage.2013.08.065

Rizzuto DS, Madsen JR, Bromfield EB, Schulze-Bonhage A, Seelig D, Aschenbrenner-Scheibe R, Kahana MJ. 2003. Reset of human neocortical oscillations during a working memory task. *Proceedings of the National Academy of Sciences* **100**:7931–7936. doi:10.1073/pnas.0732061100

Sack AT, van der Mark S, Schuhmann T, Schwarzbach J, Goebel R. 2009. Symbolic action priming relies on intact neural transmission along the retino-geniculo-striate pathway. *Neuroimage* **44**:284–293. doi:10.1016/j.neuroimage.2008.07.030

Schacter DL, Buckner RL. 1998. Priming and the Brain. *Neuron* **20**:185–195. doi:10.1016/S0896-6273(00)80448-1

Schlaghecken F, Eimer M. 2006. Active masks and active inhibition: A comment on Lleras and Enns (2004) and on Verleger, Jaśkowski, Aydemir, van der Lubbe, and Groen (2004). *Journal of Experimental Psychology: General* **135**:484–494. doi:10.1037/0096-3445.135.3.484

Schlaghecken F, Eimer M. 2002. Motor activation with and without inhibition: Evidence for a threshold mechanism in motor control. *Perception & Psychophysics* **64**:148–162. doi:10.3758/BF03194564

Schlaghecken F, Rowley L, Sembi S, Simmons R, Whitcomb D. 2007. The negative compatibility effect: A case for self-inhibition. *Advances in Cognitive Psychology* **3**:227–240. doi:10.2478/v10053-008-0027-y

Schmidt T. 2002. The Finger in Flight: Real-Time Motor Control by Visually Masked Color Stimuli. *Psychological Science* **13**:112–118. doi:10.1111/1467-9280.00421

Schroeder CE, Wilson DA, Radman T, Scharfman H, Lakatos P. 2010. Dynamics of Active Sensing and perceptual selection. *Current Opinion in Neurobiology* **20**:172–176. doi:https://doi.org/10.1016/j.conb.2010.02.010

Sereno SC. 1995. Resolution of lexical ambiguity: Evidence from an eye movement priming paradigm. *Journal of Experimental Psychology: Learning, Memory, and Cognition*. doi:10.1037/0278-7393.21.3.582

Shadmehr R, Orban de Xivry JJ, Xu-Wilson M, Shih T-Y. 2010. Temporal Discounting of Reward and the Cost of Time in Motor Control. *The Journal of Neuroscience* **30**:10507 LP-10516. doi:10.1523/JNEUROSCI.1343-10.2010

Sharma J, Sugihara H, Katz Y, Schummers J, Tenenbaum J, Sur M. 2014. Spatial attention and temporal expectation under timed uncertainty predictably modulate neuronal responses in monkey V1. *Cerebral Cortex* **25**:2894–2906. doi:10.1093/cercor/bhu086

Sohrabi A, West RL. 2009. Positive and negative congruency effects in masked priming : A neuro-computational model based on representation , attention , and conflict. *Brain Research* **1289**:124–132. doi:10.1016/j.brainres.2009.07.004

Song K, Meng M, Chen L, Zhou K, Luo H. 2014. Behavioral Oscillations in Attention: Rhythmic α Pulses Mediated through θ Band. *Journal of Neuroscience* **34**:4837–4844. doi:10.1523/JNEUROSCI.4856-13.2014

Stephan KE, Penny WD, Daunizeau J, Moran RJ, Friston KJ. 2009. Bayesian model selection for group studies. *Neuroimage* **46**:1004–1017. doi:10.1016/j.neuroimage.2009.03.025

Summerfield C, de Lange FP. 2014. Expectation in perceptual decision making: neural and computational mechanisms. *Nature Reviews Neuroscience* **15**:745–756. doi:10.1038/nrn3838

Sumner P. 2007. Negative and positive masked-priming – implications for motor inhibition. *Advances in Cognitive Psychology* **3**:317–326. doi:10.2478/v10053-008-0033-0

Sutton RS, Barto AG. 1998. Introduction to reinforcement learning. Cambridge, MA: MIT Press.

Tesche CD, Karhu J. 2000. Theta oscillations index human hippocampal activation during a working memory task. *Proceedings of the National Academy of Sciences* **97**:919–924. doi:10.1073/pnas.97.2.919

Tomassini A, Spinelli D, Jacono M, Sandini G, Morrone MC. 2015. Rhythmic Oscillations of Visual Contrast Sensitivity Synchronized with Action. *Journal of Neuroscience* **35**:7019–7029. doi:10.1523/JNEUROSCI.4568-14.2015

Tsunoda Y, Kakei S. 2011. Anticipation of future events improves the ability to estimate elapsed time. *Experimental Brain Research* **214**:323–334. doi:10.1007/s00221-011-2821-x

Tulving E, Schacter DL. 1990. Priming and human memory systems. *Science* **247**:301–306. doi:10.1126/science.2296719

968 van Vugt M, Simen P, Nystrom L, Holmes P, Cohen J. 2012. EEG Oscillations Reveal
969 Neural Correlates of Evidence Accumulation. *Frontiers in Neuroscience* **6**:106.
970 doi:10.3389/fnins.2012.00106
971 VanRullen R. 2016. Perceptual Cycles. *Trends in cognitive sciences* **20**:1–6.
972 VanRullen R. 2013. Visual attention: A rhythmic process? *Current Biology* **23**:R1110–
973 R1112. doi:10.1016/j.cub.2013.11.006
974 Verleger R, Jaśkowski P, Aydemir A, van der Lubbe RHJ, Groen M. 2004. Qualitative
975 differences between conscious and nonconscious processing? On inverse priming
976 induced by masked arrows. *Journal of Experimental Psychology: General* **133**:494–
977 515. doi:10.1037/0096-3445.133.4.494
978 Vorberg D, Mattler U, Heinecke A, Schmidt T, Schwarzbach J. 2003. Different time
979 courses for visual perception and action priming. *Proceedings of the National*
980 *Academy of Sciences* **100**:6275–6280. doi:10.1073/pnas.0931489100
981 Webster MA. 2015. Visual Adaptation. *Annual Review of Vision Science* **1**:547–567.
982 doi:10.1146/annurev-vision-082114-035509
983 Wutz A, Muschter E, van Koningsbruggen MG, Weisz N, Melcher D. 2016. Temporal
984 integration windows in neural processing and perception aligned to saccadic eye
985 movements. *Current Biology* **26**:1659–1668. doi:10.1016/j.cub.2016.04.070
986 Zion Golumbic EM, Ding N, Bickel S, Lakatos P, Schevon CA, McKhann GM, Goodman
987 RR, Emerson R, Mehta AD, Simon JZ. 2013. Mechanisms underlying selective
988 neuronal tracking of attended speech at a “cocktail party.” *Neuron* **77**:980–991.
989 doi:10.1016/j.neuron.2012.12.037
990